

## DIAGNOSIS OF TRANSVERSE COUPLING ERRORS IN A STORAGE RING\*

P. Bagley<sup>†</sup> and D. Rubin

Wilson Laboratory, Cornell University, Ithaca, New York 14850

### Abstract

In a coupled lattice excitation of either one of the two transverse normal modes will generally excite both horizontal and vertical motion at an observation point. A measurement of the relative phase and amplitude of the two components permits a partial reconstruction of the off-diagonal elements of the full turn transfer matrix. At each of the nearly 100 beam position detectors in CESR the coupled transfer matrices are measured. A fit of plausible sources of coupling to the data can improve our understanding of lattice errors and permit an optimization of the rotated quad, solenoid compensation scheme.

### Introduction

In an electron storage ring there is typically some coupling of motion between horizontal and vertical planes. Sources of the linear coupling may be rotated or skew quadrupoles or solenoidal fields. Coupling may exist due to misalignments of normal quadrupoles or as part of a compensation for the effects of an experimental solenoid. A consequence of global coupling is a shifting of the tunes of the normal modes and such a shift can be measured near the difference resonance. Local coupling is somewhat more difficult to diagnose but nevertheless may have profound impact on machine luminosity. At the interaction point which is imbedded in the longitudinal magnetic field of a solenoid a straightforward application of linear lattice theory yields a configuration of compensating skew quadrupoles that restores the ribbonlike aspect of the beams<sup>1</sup>. But errors will enlarge the vertical size of the beam and degrade luminosity. The global effects are easily identified and eliminated. Details of the evolution of the beam cross section within the insertion region are accessible by the technique described below.

### Normal Mode Decomposition

A full turn 4x4 coupled transfer matrix  $T$  can be decomposed into normal modes as follows:

$$T = VUV^{-1} \quad (1)$$

where

$$U = \begin{pmatrix} A & 0 \\ 0 & B \end{pmatrix} \quad (2)$$

$$A = \begin{pmatrix} \cos 2\pi\nu_A + a_A \sin 2\pi\nu_A & \beta_A \sin 2\pi\nu_A \\ -\gamma_A \sin 2\pi\nu_A & \cos 2\pi\nu_A - a_A \sin 2\pi\nu_A \end{pmatrix} \quad (3)$$

and similarly for B.

$$V = \begin{pmatrix} \gamma I & C \\ -C^+ & \gamma I \end{pmatrix} \text{ and } \gamma^2 + |C|^2 = 1. \quad (4)$$

T, U, and V are 4x4 matrices. A, B and C are 2x2. I is the 2x2 identity matrix. The laboratory phase space coordinates  $\mathbf{X}$  are related to the normal mode coordinates  $\mathbf{W}$  by  $\mathbf{X} = V\mathbf{W}$  where  $\mathbf{W} = (w, w', v, v')$ . Given an initial vector  $\mathbf{W}_0$ , the phase space coordinates after N turns will be  $\mathbf{W}_N = U^N \mathbf{W}_0$  and in the lab frame  $\mathbf{X}_N = V U^N \mathbf{W}_0$ . (5)

### Relative Phase and Amplitude

Consider the motion in the x-y coordinate system

\*Work supported by the National Science Foundation.

<sup>†</sup>Supported by an AT&T fellowship.

as a consequence of excitation of the  $(w, w')$  or the A mode. After some number of turns  $\mathbf{W}_N = U^N \mathbf{W}_0 = (w_N, 0, 0, 0)$ , so that the only non-zero part of the A mode vector is the  $w_N$  component. Now propagate the vector  $\mathbf{W}_N$  through some phase advance  $\phi_A$  and find the x and y displacements using (5) and (3).

$$\begin{pmatrix} x(\phi_A) \\ x'(\phi_A) \\ y(\phi_A) \\ y'(\phi_A) \end{pmatrix} = \begin{pmatrix} \gamma I & C \\ -C^+ & \gamma I \end{pmatrix} \begin{pmatrix} w_N (\cos \phi_A + a_A \sin \phi_A) \\ -w_N \gamma_A \sin \phi_A \\ 0 \\ 0 \end{pmatrix} \quad \text{and}$$

$$x(\phi_A) = \gamma w_N (\cos \phi_A + a_A \sin \phi_A) \quad \text{and} \quad (6a)$$

$$y(\phi_A) = -C_{22} w_N (\cos \phi_A + a_A \sin \phi_A) - C_{12} w_N \gamma_A \sin \phi_A. \quad (6b)$$

In general the maximum excursions of the horizontal (x) and vertical (y) motion will occur for different values of  $\phi_A = 2\pi n \nu_A$ .

The phase  $\phi_A^x$  at which x is an extremum is given by:

$$\phi_A^x = \tan^{-1} a_A. \quad (7a)$$

Similarly y is an extremum when:

$$\phi_A^y = \tan^{-1} \left( a_A + \frac{C_{12}}{C_{22}} \gamma_A \right). \quad (7b)$$

Substitution of the equations (7) into (6) yields the ratio of amplitudes:

$$\left( \frac{y}{x} \right)_A = \frac{C_{22}}{\gamma} \left[ \frac{1 + (a_A + \gamma_A \frac{C_{12}}{C_{22}})^2}{1 + a_A^2} \right]^{1/2} \quad (8)$$

The difference of equations (7b) and (7a) gives the phase difference modulo  $\pi$ .

$$\Delta \phi_A = \phi_A^y - \phi_A^x = \tan^{-1} \left[ \frac{a}{-\beta_A + a a_A} \right] \quad (9)$$

where  $a = -\frac{C_{12}}{C_{22}}$ .

Excitation of the orthogonal mode so that  $w=w'=0$  and  $v, v' \neq 0$  yields:

$$\left( \frac{x}{y} \right)_A = \frac{C_{11}}{\gamma} \left[ \frac{1 + (a_B - \gamma_B \frac{C_{12}}{C_{11}})^2}{1 + a_B^2} \right]^{1/2} \quad (10)$$

$$\Delta \phi_B = \phi_B^x - \phi_B^y = \tan^{-1} \left[ \frac{b}{-\beta_B + a a_B} \right] \quad (11)$$

where  $b = \frac{C_{12}}{C_{11}}$ .

### Thin Skew Quad

As an example consider the introduction of a thin skew quad into an otherwise decoupled lattice. The full turn transfer matrix of the unperturbed machine is

$$T = \begin{pmatrix} M & 0 \\ 0 & N \end{pmatrix} \text{ where } M = \begin{pmatrix} M_{11} & M_{12} \\ M_{21} & M_{22} \end{pmatrix}$$

(and similarly for N).

The transfer matrix for the thin skew quad is

$$S_k = \begin{pmatrix} I & S \\ S & I \end{pmatrix} \text{ and } S = \begin{pmatrix} 0 & 0 \\ 1/f & 0 \end{pmatrix}. \quad (12)$$

f is the focal length of the thin element.

$$\text{Then } T = S_k T = \begin{bmatrix} M & SN \\ SM & N \end{bmatrix} = \begin{bmatrix} M & n \\ m & N \end{bmatrix}. \quad (13)$$

#### Phase Difference

The phase difference is determined according to (9) by the ratio  $a = -C_{12}/C_{22}$ . C can be written

$$C = -\frac{m+n}{\text{tr}(A-B)\gamma}. \quad (14)$$

From (13) we have that

$$(m^+ + n) = (SM)^+ + SN = \frac{1}{f} \begin{bmatrix} M_{12} & 0 \\ N_{11} & -M_{11} & N_{12} \end{bmatrix}. \quad (15)$$

(Note that the elements of C are linear in the coupler strength.) Then

$$a = \frac{-C_{12}}{C_{22}} = \frac{0}{N_{12}} = 0 \text{ and } b = \frac{C_{12}}{C_{11}} = \frac{0}{M_{12}} = 0.$$

At the thin element  $\Delta\phi_A = \Delta\phi_B = 0$  or  $\pi$ .

#### Relative Amplitude

Equation (8) expresses relative amplitudes as

$$\left(\frac{y}{x}\right)_A = \frac{(m^+ + n)_{22}}{\text{tr}(A-B)\gamma^2} \quad (16)$$

which after some manipulation becomes

$$\left(\frac{y}{x}\right)_A = \frac{2(m^+ + n)_{22}}{[(\text{tr}(A-B))^2 + 4|m^+ + n|^{1/2} + \text{tr}(M-N)]} \quad (17)$$

The matrix elements can be written in terms of twiss parameters as:

$$\text{tr}(M-N) = 2(\cos 2\pi\nu_x - \cos 2\pi\nu_y) \quad (18)$$

$$|m^+ + n| = \frac{1}{f^2} N_{12} M_{12} = \frac{\beta_x \beta_y}{f^2} \sin 2\pi\nu_x \sin 2\pi\nu_y \quad (19)$$

$$(m^+ + n)_{22} = \frac{-1}{f} N_{12} = \frac{-\beta_y}{f} \sin 2\pi\nu_y \quad (20)$$

For a weak skew quad far from the difference resonance,

$$\text{i.e., } (2|\cos 2\pi\nu_x - \cos 2\pi\nu_y| \gg \left| \frac{\beta_x \beta_y}{f^2} \sin 2\pi\nu_x \sin 2\pi\nu_y \right|),$$

$$\left(\frac{y}{x}\right)_A \approx \frac{\frac{\beta_y}{f} \sin 2\pi\nu_y}{2(\cos 2\pi\nu_x - \cos 2\pi\nu_y)} \quad (21)$$

For a strong skew quad near the resonance

$$\left(\frac{y}{x}\right)_A \approx \left[ \frac{\beta_y \sin 2\pi\nu_y}{\beta_x \sin 2\pi\nu_x} \right]^{1/2} + \left[ \frac{\beta_y}{\beta_x} \right]^{1/2} \quad (22)$$

(It is important to keep in mind that the vertical and horizontal  $\beta$ 's are ill defined if the lattice is severely distorted due to strong coupling.)

#### Measurement

Beam position detectors are employed to measure the relative phase and amplitude of normal mode oscillations. A magnetic shaker excites one or the other of the normal modes. With the aid of a spectrum analyzer the transfer function between shaker drive signal and beam detector signal is measured. The relative phase at which maximum vertical and horizontal displacements occur, and the ratio of the maximum displacements are extracted from the transfer function. In CESR a measurement at each of the 96 beam position detectors can be completed in about an hour. Repeatability of each measurement is better than 5%.

#### Parameterization of the Data

Convenient parameters for comparison of data with theory are the elements of the C-matrix which we found to depend linearly on coupling strengths. (See equation 15.) (The linearity of C in coupler strength is not peculiar to the skew quad perturbation but persists for an arbitrary (symplectic) thin coupler.) We invert and combine equations (8) and (9) to yield:

$$-\frac{C_{12}}{C_{22}} = \frac{-\beta_A}{\cot \Delta\phi_A - a_A};$$

$$-\frac{C_{22}}{\gamma} = \left(\frac{y}{x}\right)_A (\cos \Delta\phi_A - a_A \sin \Delta\phi_A).$$

$(y/x)_A$  is the ratio of vertical to horizontal amplitudes of the A mode. The A mode reduces to the horizontal mode as the coupling vanishes. If the coupling is weak then  $|C| \ll 1$  and so  $\gamma \approx 1$ . (That  $\gamma \approx 1$  is invariably the case in any plausible CESR lattice.) Then

$$C_{22} \approx -(y/x)_A (\cos \Delta\phi_A - a_A \sin \Delta\phi_A) \quad (23)$$

$$\text{and } C_{12} \approx (y/x)_A \beta_A \sin \Delta\phi_A. \quad (24)$$

Similarly equations (10) and (11) are rearranged to give

$$C_{11} \approx (x/y)_B (\cos \Delta\phi_B - a_B \sin \Delta\phi_B) \quad (25)$$

$$\text{and } C_{12} \approx (x/y)_B \beta_B \sin \Delta\phi_B. \quad (26)$$

Note the redundancy in the measurement of  $C_{12}$ . Thus three of the four elements of the C-matrix are extracted directly from the data.

Finally the C-matrix is normalized to remove the gross dependence on the twiss parameters  $a$  and  $\beta$  according to:

$$S_g = \begin{bmatrix} \frac{1}{\sqrt{\beta_y}} & 0 \\ \frac{\alpha_y}{\sqrt{\beta_y}} & \sqrt{\beta_y} \end{bmatrix} \begin{bmatrix} C_{11} & C_{12} \\ C_{21} & C_{22} \end{bmatrix} \begin{bmatrix} \sqrt{\beta_x} & 0 \\ -\alpha_x & \frac{1}{\sqrt{\beta_x}} \end{bmatrix}. \quad (27)$$

#### CESR IR

In CESR in the vicinity of the south interaction region there is considerable local coupling due to the rotated IR quad compensation for the 1 Tesla experimental solenoid. The relative phase  $\Delta\phi_A$  is shown in Figure 1 as computed for the theoretical lattice including rotated quads and solenoid strength. (The final focus vertical and horizontal quads are rotated  $\sim 2.5^\circ$  and  $\sim 1.5^\circ$  respectively about their longitudinal axis. Weaker skew quads complete the compensation some distance into the arcs.)

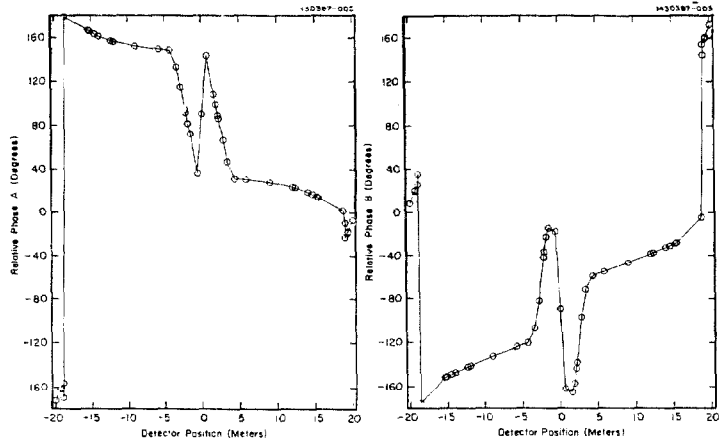


Fig. 1a. Relative phase  $\Delta\phi_A$  as a function of distance (meters) from the south interaction point.

Fig. 1b. Relative phase  $\Delta\phi_B$  as a function of distance (meters) from the south interaction point.

#### Thin Skew Quad Data

A skew quad was employed to generate a known perturbation in CESR. A skew quad located far from the interaction region was chosen to avoid confusion with

the solenoid and its compensation. Comparisons of theoretical and measured  $\Delta\phi_A$  and  $\Delta\phi_B$  are shown in Figure 2. Recall that the normalized C-matrix element  $S_{g12}$  can be measured for excitations of either of the two normal modes. The independent measurements are indicated in Figure 3 along with the theoretical prediction. The background in  $S_{g12}$  due to other coupling errors is subtracted. The consistency of the two measurements and the correspondence with the prediction are encouraging.

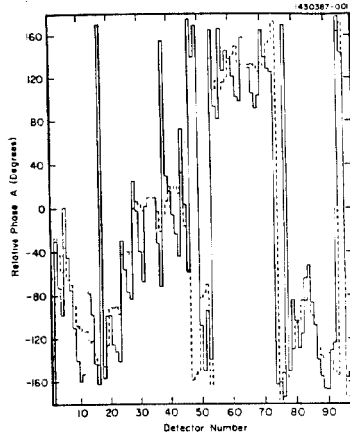


Fig. 2. Relative phase  $\Delta\phi_A$  measured (—) and computed (---) at each beam detector. The skew quad perturbation is located near detector 29. No background subtraction.

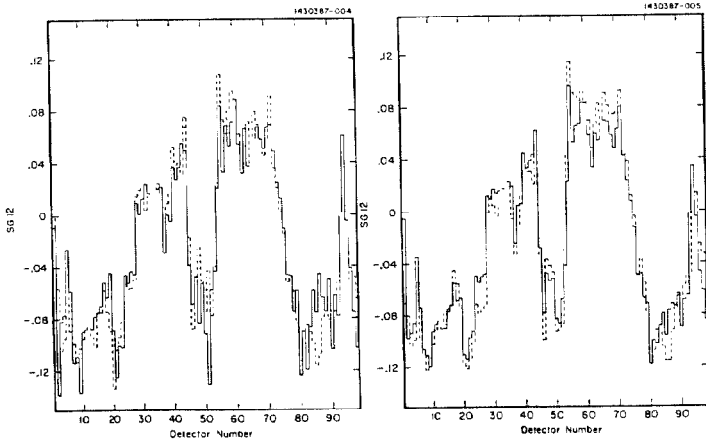


Fig 3a.  $S_{g12}$  at each beam detector measured by A mode excitation (---) and B mode excitation (—). The skew quad perturbation is near detector 29. Background is subtracted.

Fig 3b. The average of A and B mode measurements of  $S_{g12}$  (—) and the computed  $S_{g12}$  (---) at each beam detector. Perturbation at detector 29.

The  $S_{g12}$  matrix element is computed for an error in the angle of an IR REC quad and shown in Figure 4. The signal is quite distinct from that of the arc skew quad. There is some degeneracy in the  $S_{g12}$  matrix for errors in IR quads on either side of the interaction point. Fortunately the degeneracy exists only for  $S_{g12}$  and is removed with a comparison of the remaining  $S_{g12}$  elements.

#### Fitting the Data

Our goal is a capability to fit the data to plausible sources of coupling errors and then to either eliminate or compensate those errors. Sources may include errors in the rotation angles of the IR quads, errors in our approximation of the solenoid fringe field, uncertainties in the correspondence between magnetic and geometric coordinates in the

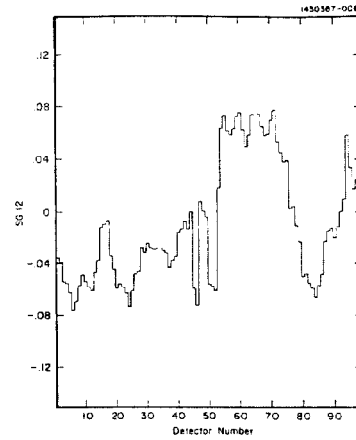


Fig 4. Computed  $S_{g12}$  at each beam detector due to an error of  $-1\text{mr}$  in the angle of the southeast REC IR quad located near detectors 1 and 96.

permanent magnet (REC) IR quads, and misalignments of arc quads or sextupoles.

Fits to simulated data yield good results. In particular, if the relative phases and amplitudes are constrained, the parameters of the fit (coupler strengths) assume appropriate values on iteration. In so far as the measurement at each of the detectors has an error of less than 5%, we can anticipate an ability to diagnose coupling errors at a level of  $\sim(1/\sqrt{N})5\% \sim 0.5\%$ .

#### Acknowledgements

The authors wish to thank the CESR operations group for developing the capability to make the measurements. For much helpful discussion we thank M. Billing and R. Littauer.

#### References

- [1] S. Peggs, "The Projection Approach to Solenoid Compensation," Particle Accelerators, vol.12, pp. 219-229, 1982
- [2] D. Edwards and L. Teng, "Parameterization of Linear Coupled Motion in Periodic Systems," IEEE Transactions on Nuclear Science, vol. NS-20, No.3, June 1973.
- [3] M. Billing, "Theory of Weakly Coupled Transverse Motion in Storage Rings," CBN 85-2.
- [4] In simulations including any reasonable coupling errors  $\gamma^{-1}$ .
- [5] S. Peggs, "Coupling and Decoupling in Storage Rings," IEEE Transactions on Nuclear Science, vol. NS-30, No.4, p. 2460, August 1983.
- [6] D. Rubin, "Solenoid Compensation in Micro-Beta Lattices," CON 84-5, March 1984.